Available online at www.sciencedirect.com
SCIENCE DIRECT®
Journal of Power Sources 119–121 (2003) 604–609
JOURNAL OF POWER SOURCES
www.elsevier.com/locate/jpowsour

Electrochemically-driven solid-state amorphization in lithium–metal anodes

Pimpa Limthongkul[a], Young-Il Jang[b], Nancy J. Dudney[b], Yet-Ming Chiang[a,*]

[a]*Department of Materials Science and Engineering, Massachusetts Institute of Technology, Cambridge, MA 02139, USA*
[b]*Condensed Matter Sciences Division, Oak Ridge National Laboratory, Oak Ridge, TN 37831, USA*

Abstract

As lithiated–metal alloys such as Li–Si or Li–Sn are of great interest as high energy density anodes for Li-ion rechargeable batteries, a fundamental understanding on how the metals behave upon lithiation is important. X-ray diffraction and HREM experiments in this work reveal that the crystallization of equilibrium inter-metallic compounds (e.g. Li–Si) is inhibited during lithiation at room temperature, and that formation of highly lithiated glass instead occurs. This glass is shown to be metastable with respect to the equilibrium crystalline phases. We show that the mechanism of electrochemical alloying is electrochemically-driven solid-state amorphization (ESA), a process closely analogous to the diffusive solid-state amorphization (SSA) of thin films. Experimental results on the diffusive reaction of Li and Si bilayer films support the proposed mechanism.

Keywords: Lithium ion rechargeable batteries; Lithium alloy anodes; Metal anodes; Amorphous phase; Silicon; Thermodynamics

1. Introduction

Metal-based anodes have received much interest as alternatives to carbon for lithium-ion rechargeable batteries due to their intrinsically high gravimetric and volumetric capacity [1–5]. Although the basic thermodynamics and electrochemistry of most of the simple alloys are known, [6,7] the fundamental material response at the micro- and nano-structural scales upon electrochemical cycling remains poorly understood.

Fracture, dislocation damage, and phase transformations are commonly observed in both cathodes and anodes subjected to electrochemical cycling in lithium-ion battery systems. Fracture can nominally be attributed to electrochemically-induced strain, and occurs in both intercalation oxides [8] and metal anodes [9]. However, metal anodes have been observed to undergo increased disorder at the atomic level upon electrochemical cycling [10–13], the cause of which has not yet been understood. In this paper, we provide direct observations of such disordering in lithiated metals with a focus on Si, using calibrated X-ray diffraction (XRD) studies and high resolution electron microscopy (HREM). A new mechanism—*electrochemically-driven solid-state amorphization* is proposed to explain this transformation from crystalline to disordered phases. Supporting evidence is also demonstrated in a conventional Li–Si bilayer.

2. Experimental procedure

Electrodes for electrochemical testing were prepared by mixing an electrochemically active Si (−325 mesh, 99.5% Alfa Aesar) and a non-reactive internal standard of fine nickel powder (0.08–0.15 μm, 99.8% Alfa Aesar) with polyvinylidene fluoride binder, PVDF (534,000 M_w, Aldrich) in a 6:3:1 weight ratio, using γ-butyrolactone (+99%, Aldrich) as the solvent, in an Ar-filled glovebox with <3 ppm oxygen and H_2O. The non-reactive Ni powder acted as a conductive additive and also allowed the amount of crystalline silicon phase present in the tested sample to be quantified in the X-ray diffraction experiments. The powder–binder mixture was dried, pressed into 1/4 in. diameter pellets of ∼100 μm thickness, and assembled in a standard stainless steel electrochemical cell with Teflon™ insulator. The pellets were tested as the positive electrode against Li foil (0.75 mm thick, Alfa Aesar), using Celgard 2400™ (Celgard Inc.) as the separator. The electrolyte used was a 1 M solution of $LiPF_6$ in a 1:1 (w/w) EC:DMC mixture (EM

* Corresponding author. Tel.: +1-617-253-6471; fax: +1-617-253-6201.
E-mail address: ychiang@mit.edu (Y.-M. Chiang).

0378-7753/03/$ – see front matter © 2003 Elsevier Science B.V. All rights reserved.
doi:10.1016/S0378-7753(03)00303-3

Science). The electrochemical tests were carried out at room temperature at a constant current density of 10 mA/g of active metal.

X-ray diffraction (Rigaku, RU300, Cu Kα radiation) was performed before and after lithiation of the sample. The known amount of Ni in the starting mixture served as a reference standard from which the relative amounts of crystalline phases after lithiation were quantified [14]. High resolution and analytical electron microscopy experiments were performed using a JEOL 2010FX TEM (JEOL Ltd.) operating at 200 keV and equipped with an energy-dispersive X-ray detector (Link Systems). All handling of the samples for the XRD and HREM experiments, as well as loading of the sample into the TEM specimen holder, was conducted in the Ar-filled glovebox with <30 s exposure to air.

In order to make a direct comparison with the electrochemically alloyed samples to the same reactants in a conventional thin film geometry, Si films of 0.5 μm thickness were deposited on polycrystalline Al_2O_3 plates by dc magnetron sputtering of a Si target (99.999%, Kurt J. Lesker) in Ar atmosphere. To ensure crystallinity, the Si films were annealed at 1000 °C for 10 h in Ar. Li films of 1.5 μm were then deposited on the Si films by thermal vapor deposition of Li metal at temperature ~50–80 °C, to obtain a bilayer with overall Li/Si molar ratio of 2.82. The bilayer films were packaged under a layer of lithium phosphorous oxynitride (Lipon) [15] of 0.2 μm thickness, deposited by rf magnetron sputtering of Li_3PO_4 in N_2 atmosphere. Between the Li and Li_3PO_4 depositions, the samples were handled in an Ar-filled glovebox.

3. Results and discussion

3.1. Electrochemical and microstructural characterization

Fig. 1 (solid line) shows a voltage profile of a Si powder sample lithiated to a total charge capacity of 1280 mAh/g (Li/Si molar ratio of 1.34, or 57 mol% Li). This composition clearly lies within the equilibrium $Li_{12}Si_7$–Si two-phase field. The flat voltage plateau at 0.1 V suggests a two-phase field of constant lithium chemical potential. The equilibrium voltage over this composition range was measured by interrupting this test at 200 mAh/g capacity intervals and holding for 4 h, whereupon the cell voltage relaxes to a steady-state value of 0.18 V (Fig. 1, dashed line). From the results of Wen and Huggins [16], if co-existence of the equilibrium crystalline phases Si and $Li_{12}Si_7$ were to occur, an equilibrium voltage of ~0.34 V with respect to pure Li metal would be expected. However, the lower equilibrium voltage in our experiment indicates a significant deviation from thermodynamic equilibrium Li–Si phase formation.

Fig. 2a and b compare X-ray diffractograms of the Ni and Si powder mixture before and after lithiation. If equilibrium

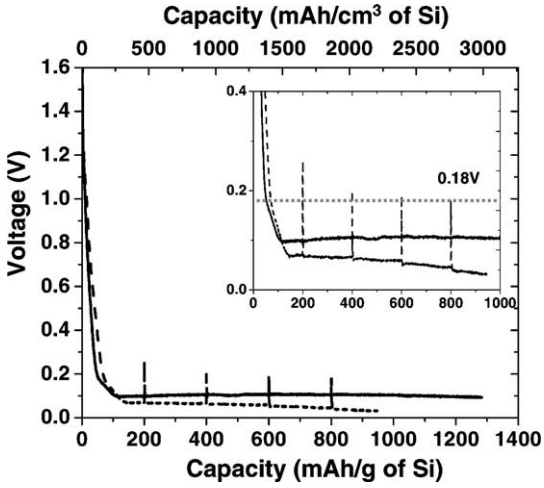

Fig. 1. Voltage profile shown in a solid line for crystalline Si sample lithiated to 1280 mAh/g (1.34 mol of Li/mol of total Si, 57 mol% Li/total Si). The voltage profile of another cell whose voltage is allowed to reach the equilibrium voltage is shown as a dashed line. A voltage plateau appears at a much lower voltage than expected for equilibrium Li_2Si_7–Si co-existence (0.34 V).

were maintained along this composition trajectory, $Li_{12}Si_7$ should crystallize and increase in relative fraction while co-existing with crystalline Si. Fig. 2b does show a decrease in the Si phase reflections relative to the Ni reference, from which it was determined that 38 mol% of the starting silicon phase remained. However, no new reflections of any crystalline phase appeared. By comparing the peak intensity of the remaining crystalline Si to the Ni reference and from the total lithium transported (Fig. 1), the average Li/Si molar ratio of the Li–Si amorphous reaction product was calculated to be 2.17 (68 mol% Li, or a composition $LiSi_{0.47}$). This composition is shown as the terminal composition along the trajectory in Fig. 3.

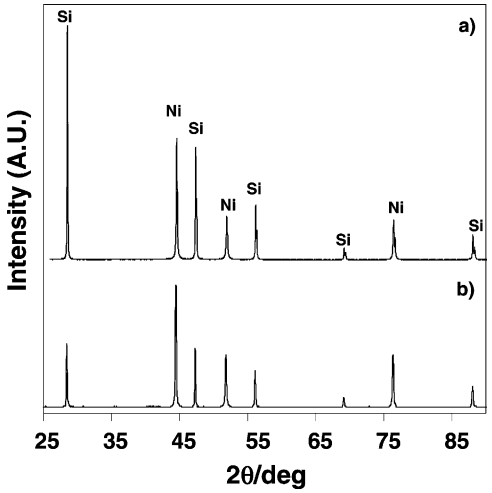

Fig. 2. X-ray diffraction experiment using Ni as an internal standard to calibrate the fraction of remaining crystalline Si upon electrochemical lithiation. (a) The starting mixture of Si:Ni:PVDF (60:30:10 (w/w)); (b) Si sample lithiated to 57 mol% Li/total Si. No new crystalline phases accompany the decrease in Si fraction in (b).

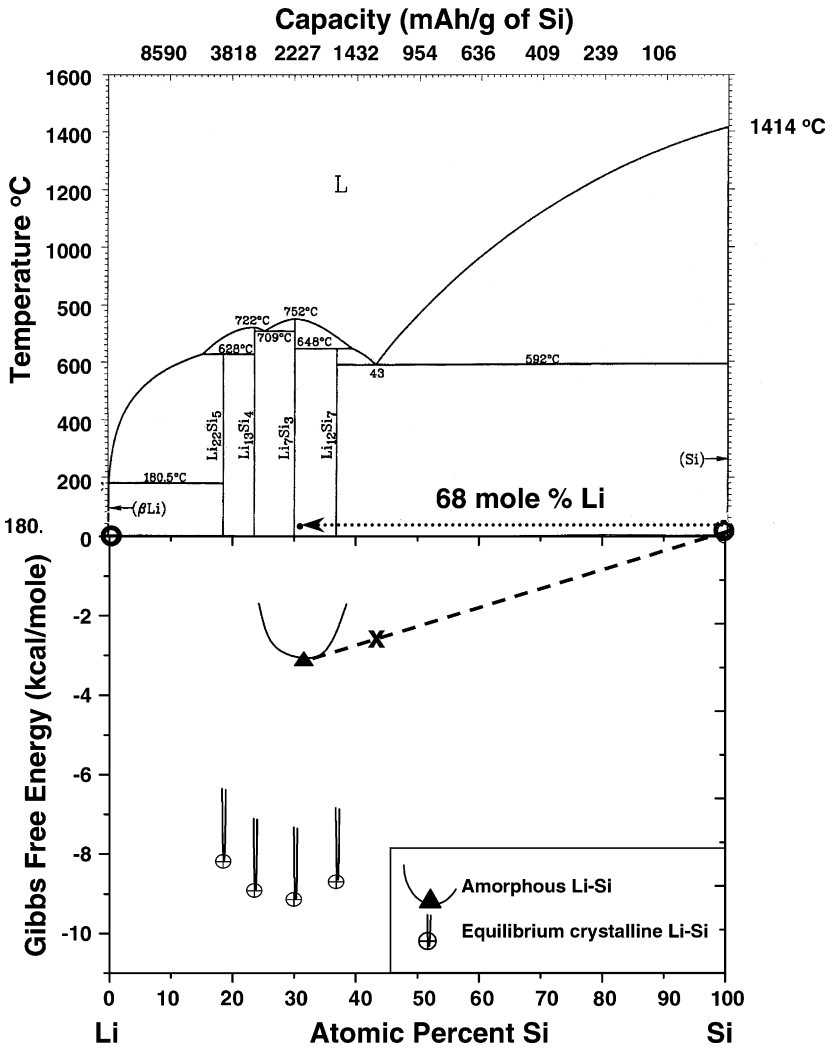

Fig. 3. (Top) Equilibrium Li–Si phase diagram [21], and (bottom) Gibbs free energy diagram for known crystalline phases and amorphous Li–Si alloy identified in this work. The overall composition of an electrochemically lithiated sample showing co-existence of crystalline Si and the metastable amorphous phase is denoted by X. When crystallization of the equilibrium intermetallic compounds is suppressed, electrochemically-induced solid-state amorphization instead occurs at room temperature. See text for details.

High resolution and analytical electron microscopy showed that the microstructure of the sample was dominated by amorphous-phase particles. The composition of the particles was found via energy-dispersive X-ray analysis (EDX) to be Si-rich. Fig. 4 shows the HREM bright field images, corresponding dark field images, a typical selected-area diffraction pattern, and an energy-dispersive spectrum typical of the amorphous phase particles. The bright-field images (Fig. 4a and c) showed a periodic contrast with no lattice fringes; the electron diffraction patterns showed diffuse rings; and the dark field images (Fig. 4b and d) formed using the diffracted intensity from the first diffuse ring showed homogeneous scattering intensity and no sign of strongly diffracting regions larger than a few Angstroms. These observations indicate the absence of crystalline phases. The EDX spectrum showed predominantly Si; Li is not detectable with the detector used. The low oxygen concentration in these amorphous phase rules out the two most likely artifacts possible in this experiment, possible oxidation of the Si forming amorphous silicon oxides and amorphous reaction products of the alloy with organic electrolyte. Most of the particles analyzed by HREM were of this type, although some crystalline Si particles were also observed; this is consistent with the XRD results. In some cases, the co-existence of an amorphous phase with a central core of crystalline Si was observed in a single particle. Thus, the physical co-existence of an amorphous phase and crystalline silicon was confirmed, consistent with the constant lithium chemical potential implied by the voltage plateau in Fig. 1.

3.2. Electrochemically-driven solid-state amorphization

As the experimental data has shown, the Li–Si system above forms an amorphous Li–Si phase upon electrochemical lithiation. This transformation from a crystalline to a

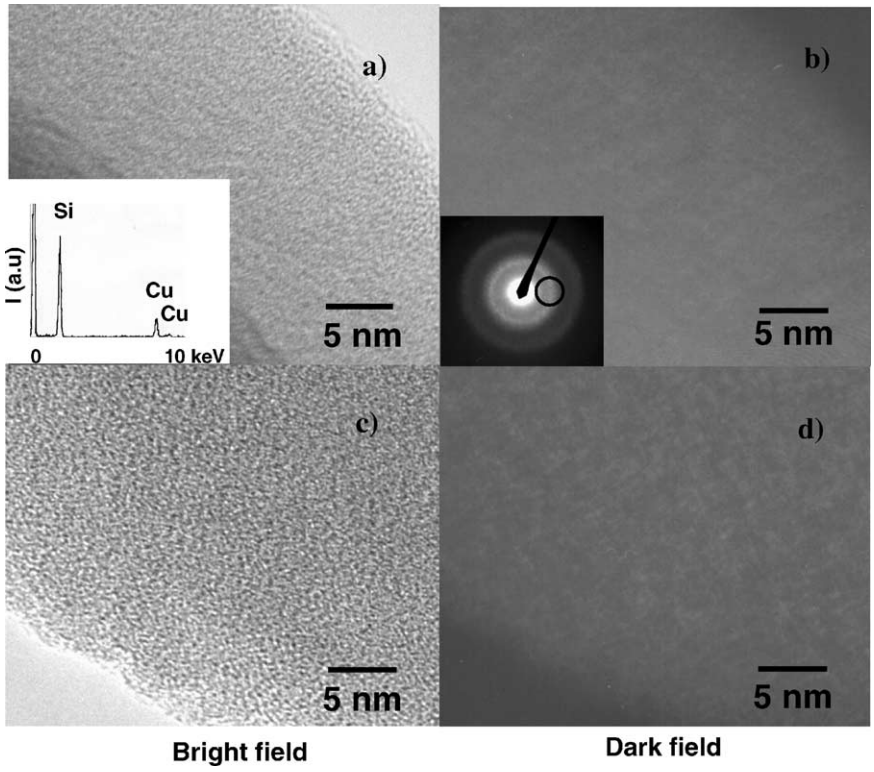

Fig. 4. (a and c) HREM bright field images; and (b and d) their corresponding dark field images showing microstructure of Si after lithiation to 68 mol% Li, showing that electrochemical lithiation has resulted in the production of an amorphous alloy.

disordered phase can be explained in the context of electrochemically-driven solid-state amorphization (ESA). Solid-state amorphization (SSA) is a phenomenon in which formation of amorphous materials occurs by a solid-state reaction rather than upon quenching from the melt. Although, to our knowledge, electrochemically-driven solid-state amorphization has not been discussed in the literature, solid-state amorphization through diffusive reaction has been known for 20 years in bilayer or multilayer thin films systems, in which the film thickness is comparable to an interface thickness [17]. Amorphization occurs when a thermodynamically preferred crystalline intermediate compound is unable to nucleate, and a glassy phase that is metastable yet lower in free energy than the pure reactants forms instead. We propose that a similar phenomenon can occur when alloying is electrochemically-driven. The basic criteria necessary for transformation from a crystalline to amorphous state, bypassing the equilibrium intermediate compound, is a negative heat of mixing, large size differences between atoms, high alloying concentration, and large differences in diffusivities of atoms [17–24]. The negative heat of mixing provides the driving force for mixing while the other criteria are typically associated with a large nucleation barrier and instability of the new crystalline phases. Although thin-film solid-state amorphization has not previously been studied in any Li–Me alloy (Me is a metal that can alloy with Li such as Si, Sn, Al, Ag, Sb, and Zn), these criteria are easily met in various Li–Me systems. The Li–Si phase diagram (Fig. 3, top) [25] exhibits numerous intermetallic phases, the nucleation and growth of which must be avoided if solid-state amorphization is to occur. The fact that the intermediate compounds have complex crystal structures [25] with little structural similarity to the pure end members was expected to help frustrate crystallization of Si upon alloying with Li, since continuous transformation of, or epitaxial growth on, the parent phases is unlikely.

Table 1 lists available standard free energies of formation of the pure metals as well as the equilibrium crystalline intermetallic compounds in Fig. 3 [26,27]. Combined with the electrochemical test data from this work for the amorphous Li–Si phase, we construct in Fig. 3 (bottom) a Gibbs free energy diagram for all presently known crystalline phases in this system and the amorphous phase. The standard

Table 1
Standard Gibbs free energies of for Li at 25 °C [26], Si at 25 °C [26] and Li–Si alloys at 415 °C, [27] and amorphous Li–Si alloy at 25 °C from the present work

Phases	G_i (kcal/mol)
Li	−2.072
$Li_{12}Si_7$	−199.516
Li_7Si_3	−109.944
$Li_{13}Si_4$	−183.956
$Li_{22}Si_5$	−273.375
Amorphous $LiSi_{0.47}$ (this work)	−4.151
Si	−1.341

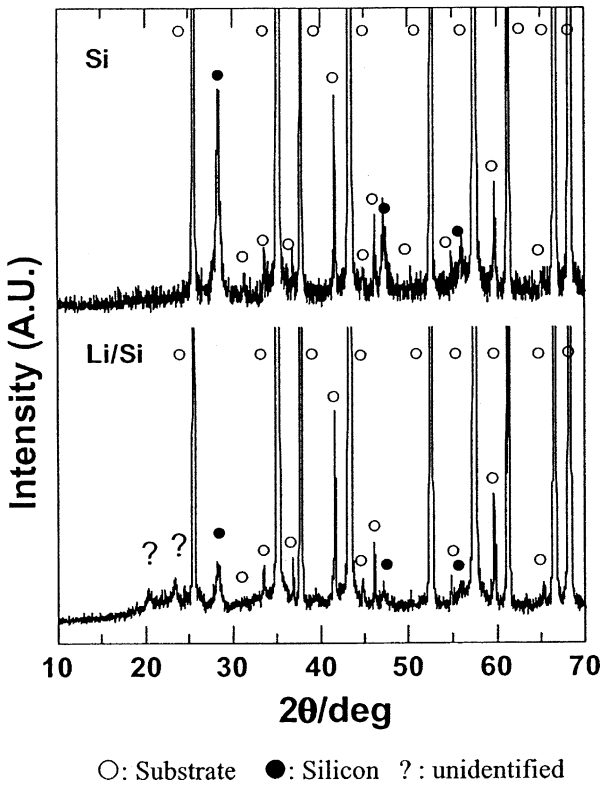

Fig. 5. X-ray diffraction from the thin film solid-state reaction of Li with Si at a molar ratio of 2.82 Li/Si (74 mol% Li). Diffractogram of starting Si film is shown at the top. The substrate is Al_2O_3. At the bottom, results from the Li–Si bilayer formed by thermal evaporation of Li at 50–80 °C onto the Si film showed none of the expected equilibrium crystalline Li–Si compounds associated with this overall composition.

Gibbs free energy of pure Li and Si shown are the data at 298 K (±3 K). The equilibrium Li–Si crystalline phases are treated as line compounds as shown in the phase diagram (Fig. 3), and their Gibbs energies are calculated from the values in Table 1 for the respective formula units Li_xSi_y, where $x + y = 1$. Although experimental thermodynamic data are only available for these compounds at a temperature of 688 K (415 °C), the formation free energies are likely to vary by less than 1% between 688 K and room temperature. For the amorphous phase, the composition was assumed to be $LiSi_{0.47}$, as determined from the diffraction analysis and electrochemical test. Its free energy was determined using the Nernst equation, $\Delta G^{\circ}_{LiSi_{0.47}} = -nFV = -4.15$ kcal/mol, where V is the experimental equilibrium voltage of the amorphous alloy with respect to pure lithium, F is the Faraday's constant, and n is the number of electrons transported per Li^+, equal to unity.

The free energy construction (Fig. 3) is consistent in every aspect with the experimental observations. The crystalline intermetallics are the thermodynamically stable phases having much lower Gibbs energy than the amorphous alloy. However, since these phases clearly do not easily crystallize at room temperature, as the silicon is lithiated, the metastable Li–Si phase forms, crystalline Si and the amorphous Li–Si phase of approximately constant composition coexist. This is consistent with the long voltage plateau observed in the electrochemical test. The XRD results confirm that the only crystalline phase present (aside from the non-reactive internal standard) is Si, and the HREM results show only crystalline Si and the amorphous Si-containing phase. The co-existence of an SSA-produced amorphous phase and a crystalline phase has previously been observed in thin film reactions, one example being the Au–La thin film system [17].

3.3. Thin-film solid-state amorphization in Li–Si

Thin-film bilayer experiments showed that in this system, solid-state reaction between Li and Si thin films occurs readily at 50–80 °C. The overall Li/Si molar ratio of this diffusion couple is 2.82. The XRD results of the Si film before deposition, and after Li film deposition are shown in Fig. 5. A reduction in Si integrated peak intensity of about a factor of 4 is observed. However, as in the electrochemical lithiation experiments, no peaks were found that could be associated with any of the equilibrium Li–Si crystalline phases. Minor peaks from unidentified phase(s) are seen in Fig. 5. These peaks, which were not seen in the electrochemically-alloyed samples, could correspond to a Li–Si metastable phase that formed due to a higher reaction temperature during Li deposition (50–80 °C). The majority reaction product appears to be amorphous. It is not surprising that Li–Si thin films react readily at temperature below 80 °C, given the rapid Li transport rate at room temperature (necessary for these alloys to function electrochemically at room temperature). In related work, we have seen rapid reaction at the same temperature range in Li–Sn thin film couples as well. Electron microscopy was not accomplished on these samples due to the difficulty of preparing electron-transparent foils of highly lithiated alloys without oxidation. The results nonetheless demonstrate the close analogy between electrochemically-driven and conventional thin-film solid-state amorphization reactions, and that solid-state reaction at temperatures close to room temperature in Li–Me systems can result in a metastable phase. Additional details of this work, and results on related lithium–metal systems, are discussed in [28].

4. Conclusions

In this work, the microscopic reaction mechanism occurring when metals are electrochemically lithiated at room temperature has been studied. Using Li–Si as a model system, direct and indirect experimental observations via calibrated XRD, HREM and electrochemical testing have revealed that formation of metastable non-crystalline phases can readily occur at room temperature in Si subjected to electrochemical lithiation. This phenomenon has been described as *electrochemically-driven solid-state amorphization*, during which a metal is amorphized upon alloying

with Li during electrochemical cycling. A self-consistent thermodynamic interpretation is presented to explain the above process. The Li–Si bilayer thin films were similarly found to react without forming any of the expected equilibrium crystalline phases, suggesting that Li–Me alloys in general are likely candidates for solid-state amorphization.

Acknowledgements

The authors thank W. Craig Carter and John B. Vander Sande for helpful discussions. Funding and instrumentation in the Shared Experimental Facilities at MIT were supported by NSF Grant no. 9400334-DMR. Support for Y.I. Jang and N.J. Dudney was provided by the US Department of Energy's Division of Materials Sciences and Division of Chemical Sciences under contract DE-AC05-00OR22725 with the Oak Ridge National Laboratory, managed by UT-Battelle, LLC.

References

[1] J. Yang, M. Wachtler, M. Winter, J.O. Besenhard, Electrochem. Solid-State Lett. 2 (1999) 161.
[2] R.A. Huggins, J. Power Sources 26 (1989) 109.
[3] Y. Idota, T. Kubota, A. Matsufuji, Y. Maekawa, T. Miyasaka, Science 276 (1997) 1395.
[4] I.A. Courtney, J.R. Dahn, J. Electrochem. Soc. 144 (1997) 2045.
[5] O. Mao, R.L. Turner, I.A. Courtney, B.D. Fredericksen, M.I. Buckett, L.J. Krause, J.R. Dahn, Electrochem. Solid-State Lett. 2 (1999) 3.
[6] A. Anani, S. Crouchbaker, R.A. Huggins, J. Electrochem. Soc. 134 (1987) 3098.
[7] Y. Geronov, P. Zlatilova, G. Staikov, J. Power Sources 12 (1984) 155.
[8] H. Wang, Y.-I. Jang, B.Y. Huang, D.R. Sadoway, Y.-M. Chiang, J. Electrochem. Soc. 146 (1999) 473.
[9] P. Limthongkul, H. Wang, Y.-M. Chiang, in: Proceedings of the 200th Meeting of the Electrochemical Society, Symposium on Rechargeable Batteries, San Francisco, 2001.
[10] J. Yang, M. Winter, J.O. Besenhard, Solid State Ionics 90 (1996) 281.
[11] Y. Hamon, T. Brousse, F. Jousse, P. Topart, P. Buvat, D.M. Schleich, J. Power Sources 97–98 (2001) 185.
[12] G.W. Zhou, H. Li, H.P. Sun, D.P. Yu, Y.Q. Wang, X.J. Huang, L.Q. Chen, Z. Zhang, Appl. Phys. Lett. 75 (1999) 2447.
[13] B. Gao, S. Sinha, L. Fleming, O. Zhou, Adv. Mater. 13 (2001) 816.
[14] B.D. Cullity, Elements of X-ray Diffraction, Addison-Wesley Publishing Co., Reading, MA, 1978.
[15] X. Yu, J.B. Bates, G.E. Jellison Jr., F.X. Hart, J. Electrochem. Soc. 144 (1997) 524.
[16] C.J. Wen, R.A. Huggins, J. Solid State Chem. 37 (1981) 271.
[17] R.B. Schwarz, W.L. Johnson, Phys. Rev. Lett. 51 (1983) 415.
[18] T.R. Anantharaman, Materials Science Surveys, no. 2, Trans Tech Publications, USA, 1984, p. 2.
[19] W.L. Johnson, in: S. Yip (Ed.), Materials Interfaces: Atomic-level Structure and Properties, Chapman & Hall, New York, 1992, p. 516.
[20] C. Lin, G.W. Yang, B.X. Liu, Phys. Rev. B 61 (2000) 15649.
[21] T. Egami, J. Non-Cryst. Solids 207 (1996) 575.
[22] T. Egami, Mater. Sci. Eng. Part A: Struct. Mater. Properties Microstruct. Process. 226 (1997) 261.
[23] H.S. Chen, K.A. Jackson, Metallic glasses, in: Proceedings of Papers Presented at the Seminar of the Materials Science Division of the American Society for Metals, 18–19 September 1976, American Society for Metals, Metals Park, OH, 1978, p. 74.
[24] D.E. Polk, B.C. Giessen, Metallic glasses, in: Proceedings of Papers Presented at the Seminar of the Materials Science Division of the American Society for Metals, 18–19 September 1976, American Society for Metals, Metals Park, OH, 1978, p. 1.
[25] H. Okamoto, in: T.B. Massalski (Ed.), Binary Alloy Phase Diagram, ASM International, Materials Park, OH, 1990, p. 2465.
[26] I. Barin, G. Platzki, Thermochemical Data of Pure Substances, VCH, Weinheim, New York, 1995.
[27] A.A. Anani, R.A. Huggins, J. Electrochem. Soc. 134 (1987) C407.
[28] P. Limthongkul, Y.-I. Jang, N.J. Dudney, Y.-M. Chiang, Acta Mater. 51 (2003) 1103–1113.